Article

Chinese Science Bulletin

Condensed Matter Physics

February 2011 Vol.56 No.4-5: 372–375
doi: 10.1007/s11434-010-4291-0

Stable structure of $Zr_{49}Cu_{44}Al_7$ metallic glass matrix composite with CuZr phase under high pressure up to 40.8 GPa

LI Gong[1*], LIU RiPing[1], LI YanChun[2] & LIU Jing[2]

[1] *State Key Laboratory of Metastable Materials Science and Technology, Yanshan University, Qinhuangdao 066004, China;*
[2] *Beijing Synchrotron Radiation Laboratory, Institute of High Energy Physics, Chinese Academy of Sciences, Beijing 100039, China*

Received July 13, 2010; accepted August 26, 2010

Ternary $Zr_{49}Cu_{44}Al_7$ metallic glass matrix composite rods with CuZr nano-phase, exhibiting an elastic strain of 1.6% and a high strength of 1.78 GPa, have been manufactured. The structural evaluation of the ternary metallic glass matrix composite under high pressure has been investigated using angle dispersive X-ray diffraction with a synchrotron radiation source. The investigation shows that the amorphous matrix structure is stable under pressures up to 40.8 GPa at room temperature. No pressure induced CuZr nano-phase disappearing or growing was detected. According to the Bridgeman equation of state, the bulk modulus B_0 =115.2 GPa has been obtained.

$Zr_{49}Cu_{44}Al_7$ metallic glass matrix composite, high pressure, strength

Citation: Li G, Liu R P, Li Y C, et al. Stable structure of $Zr_{49}Cu_{44}Al_7$ metallic glass matrix composite with CuZr phase under high pressure up to 40.8 GPa. Chinese Sci Bull, 2011, 56: 372–375, doi: 10.1007/s11434-010-4291-0

Compared with the with other bulk metallic glasses (BMGs) [1–4], Zr-Cu-Al ternary alloys have better combinations of high strength, good ductility and low production costs [5–7]. It has recently been discovered that the mechanical properties of Zr-Cu-Al ternary BMG are sensitive to their microstructures [8]. For instance, Fan et al. [9], Yan et al. [10] and Hui et al. [11] have investigated the compressive fracture characteristics, crystallization behavior and atomic structures of Zr-based bulk metallic glasses and Li et al. [12] have explored the microstructure of CuZrTi bulk metallic glass. It has been revealed that ternary $Zr_{47.5}Cu_{47.5}Al_5$ monolithic BMG exhibits a large plastic strain (16%), as well as "work hardening" behavior, upon compression [13,14]. Furthermore, nano-structure composites in Zr-based BMG [15] have been designed to improve the toughness and tensile ductility in bulk metallic glass at room temperature. Mechanically (pressure) induced crystallization has been observed in many BMG systems [16–18] and the effects of crystallization fractions on the mechanical properties of Zr-based metallic glass matrix composites have been studied by Qiu et al. [19]. Because thermodynamic variables, such as temperature and pressure, can have a significant effect on the chemical and physical properties of matter, it is important to investigate the structure of solid matter under high pressure [20]. Ma et al. [21] and Han et al. [22] have researched the effects of additives on diamond single crystals synthesized under HPHT and Zang et al. [23] and Zhou et al. [24] have studied the growth mechanism of the diamond-to-graphite transformation under diamond-stable and HPHT conditions. In previous work, we have reported the compression behavior of a ternary BMG [25]; however, little is known about metallic glass matrix composites under high pressure. In this paper, we have investigated the compression behavior of $Zr_{49}Cu_{44}Al_7$ metallic glass matrix composite. We have manufactured bulk $Zr_{49}Cu_{44}Al_7$ metallic glass matrix composite rods, 8 mm in diameter, using copper mold casting techniques and have unraveled the compression behavior of this new alloy under high pressure at room temperature using angle dispersive X-ray diffraction with a synchrotron radiation source. Finally, we have

*Corresponding author (email: gongli@ysu.edu.cn)

obtained the equation of state of this system.

1 Experimental

We have prepared the master alloy using an arc-melting technique under a Ti-gettered argon atmosphere with high-purity elements (99.8% Zr, 99.99% Al and 99.99% Cu). To ensure even distribution of the alloying elements, the master alloy was melted several times in succession and then cast into amorphous rods, up to 8 mm in diameter, by the suction casting method. We have ascertained the nature of the structure of bulk $Zr_{49}Cu_{44}Al_7$ metallic glass matrix composites using X-ray diffractometry (Rigaku, CN2301) with a monochromatic CuKα radiation source. We have studied the thermal stability of the alloy, specifically the glass transition temperature and the crystallization behavior, with a Nestzsch STA449C differential scanning calorimeter (DSC) in a calibrated high-temperature calorimeter under pure Ar gas flowing at different heating rates.

We have conducted compressive testing of the as-cast cylindrical rods at room temperature using a Gleeble 1500 hot simulator at a constant strain rate of 10^{-1} s^{-1} with no holding time. The fracture morphology has been investigated using an Oxford scanning electron microscope operating at 20 kV.

For the pressure experiments, we have carefully scraped powder from bulk $Zr_{49}Cu_{44}Al_7$ metallic glass matrix composite rods using 4Cr13 stainless steel scalpels. The pressure was generated using a diamond anvil cell (DAC), where the culet of the diamond anvil has a diameter of 400 μm. We then loaded the amorphous powder sample, together with the pressure-calibrator ruby, into a 120 μm-diameter hole of a T301 stainless steel gasket, which was prepared with a thickness of about 40 μm. Silicone oil was used as the pressure-transmitting media. The *in-situ* angle dispersive X-ray diffraction (ADXRD) measurements were carried out in Beijing Synchrotron Radiation Laboratory (BSRL). The Debye rings were recorded using an image plate in transmission mode and the XRD patterns were integrated from the images using FIT2d software [26]. The X-ray beam diameter was 45 μm ×26 μm. A Li detector was used to collect the diffraction signal under various pressures. We have determined the experimental pressure from the position of the diffraction peak of ruby.

2 Results and discussion

Shown in Figure 1 are the X-ray diffraction pattern, the DSC curve for different scanning rates and the optical micrograph for an 8 mm diameter specimen. Each broad peak near 38° is superimposed with a small crystalline peak, which has been identified as predominantly the CuZr phase, as shown in Figure 1(a). The inset of Figure 1(a) shows the optical micrograph of the central areas of a $Zr_{49}Cu_{44}Al_7$ metallic glass matrix composite rod. We have observed dense, dot-shaped crystalline phases, which are consistent with XRD results (see Figure 1(a)). According to the DSC curve shown in Figure 1(b), as the heating rate increases, the exothermic peak positions of the DSC traces shift obviously towards higher temperatures. For a heating rate of 20 K/min, for example, the glass transformation temperature (T_g) is 720 K and the on-set (T_x) and peak temperatures of crystallization (T_p) are 779 and 781 K, respectively.

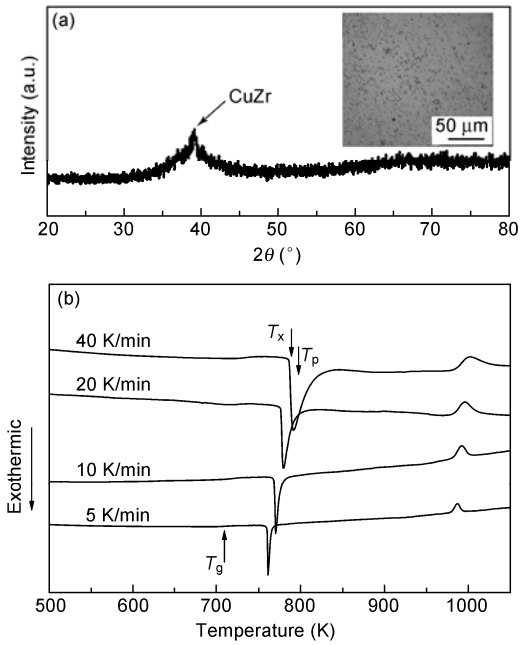

Figure 1 (a) An XRD pattern for the as-cast $Zr_{49}Cu_{44}Al_7$ metallic glass matrix composite. The inset shows the optical micrograph of the central areas of $Zr_{49}Cu_{44}Al_7$ metallic glass matrix composite rod. (b) DSC curves for the as-cast metallic glass matrix composite taken at different heating rates.

A typical example of the stress-strain curves that we have obtained is shown in Figure 2, where the strain rate is 10^{-1} s^{-1}. As shown in Figure 2, $Zr_{49}Cu_{44}Al_7$ metallic glass matrix composite rods exhibited a high failure stress of 1.78 GPa at room temperature. After reaching the maximum stress, the stress dropped to zero value immediately, which is typical of "brittle" failure. The failed surface exhibited a "vein-like" pattern on the recovered specimens. The inset of Figure 2 shows the macroscopic appearance of the $Zr_{49}Cu_{44}Al_7$ metallic glass matrix composite specimen after testing at room temperatures. Consistent with ZrTiCuNiBe BMG [27], catastrophic failure of the bulk amorphous specimen resulted in a flat macroscopic fracture that occurred along a plane, oriented 45° to the loading axis, at room temperature. At room temperature, $Zr_{49}Cu_{44}Al_7$ metallic glass matrix composite behaves like a typical brittle solid material. The fracture occurred along the maximum shear plane, which is declined by 45° from the direction of the applied load. At the fracture surface, we have observed a crack with a serrated

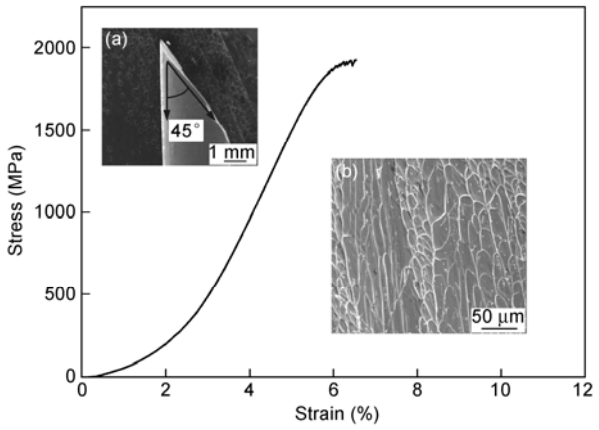

Figure 2 Stress-strain curve for the as-cast $Zr_{49}Cu_{44}Al_7$ metallic glass matrix composite. Inset (a) shows the macroscopic fracture pattern at room temperature. Inset (b) shows the vein pattern on the fracture surface.

edge on the ridge of the veins.

To further understand the mechanical behavior, we have carried out high pressure experiments at BSRL. Figure 3 shows the synchrotron radiation X-ray diffraction spectrum under different pressures in the $Zr_{49}Cu_{44}Al_7$ alloy. As the pressure increases, the broad diffusive amorphous hole (marked with a dotted line) and the superimposed small crystalline peak (marked with an arrow) shift obviously to higher angles, which illustrates the compression behavior of the alloy. We have detected no new diffraction peaks from the curves between 0 and 40.8 GPa, which implies that the structure is quite stable at room temperature. To gain a fuller understanding of the $Zr_{49}Cu_{44}Al_7$ composite behavior at high pressures, we have obtained the equation of state (EOS). Bridgeman has presented the EOS as follows [28]:

$$-\Delta V/V_0 = a_0 + aP + bP^2 + cP^3 + \cdots\cdots \quad (1)$$

where V_0 is the volume at zero pressure, and the coefficients a_0, a, b and c can be determined using the least squares method. The relative volume change $\Delta V/V_0$ can be derived directly from the relative density change. Because the synchrotron radiation X-ray diffraction peak positions reflect changes in atomic density [29], it is instructive to convert the spectrum in Figure 3 into a plot of relative volume changes versus pressure, which is shown in Figure 4, where the density has been determined using the position of the first peak [30,31]. We have estimated the relative volume change $\Delta V/V_0$ ($\Delta V=V_P-V_0$) at a given pressure (V_P) to that at zero pressure (V_0). Finally, we have fit the experimental $\Delta V/V_0$-P data to the Bridgeman EOS, which can be expressed as

$$-\Delta V/V_0 = 4.96\times10^{-4}+0.00868P - 0.000246P^2+0.00000342P^3. \quad (2)$$

From this equation, we have obtained the bulk modulus B_0 according to the relationship, $B_0=1/a$. The bulk modulus B_0 is found to be 115.2 GPa. Because a higher bulk modulus indicates a harder material, it is understandable that the compressibility is lower (~15%) in this system.

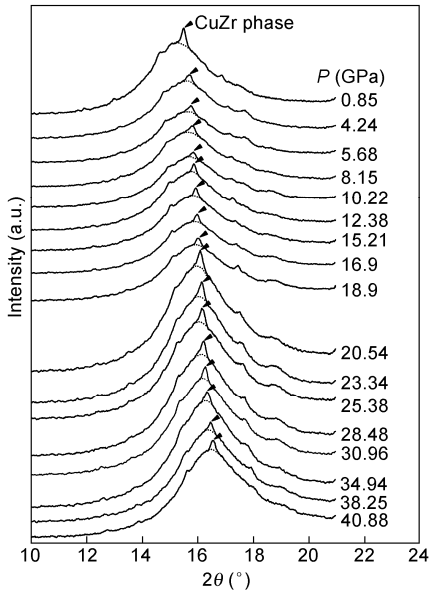

Figure 3 Angle-dispersion X-ray diffraction patterns of $Zr_{49}Cu_{44}Al_7$ metallic glass matrix composite at various pressures. The amorphous hole is marked with a dotted line and the small crystalline peak is marked with an arrow.

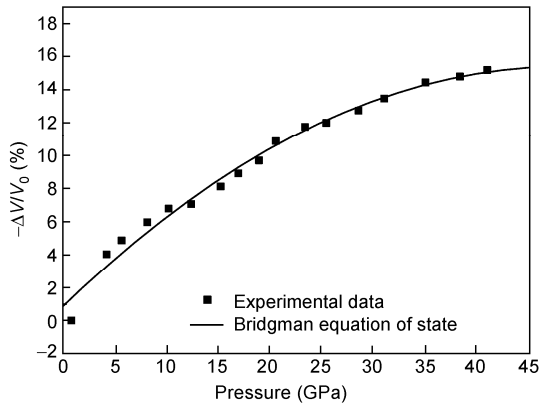

Figure 4 Pressure dependence of relative volumetric changes in $Zr_{49}Cu_{44}Al_7$ metallic glass matrix composite at room temperature.

3 Conclusions

A new ternary $Zr_{49}Cu_{44}Al_7$ metallic glass matrix composite with a diameter of 8 mm has been manufactured by copper mold casting. We have determined the glass transition temperature and the crystallization peak temperature to be 720 K and 781 K, respectively. This metallic glass matrix composite exhibited poor plastic deformation, yet it proved to have a high strength of about 1.78 GPa. The compression behavior at room temperature, using *in-situ* high pressure angle dispersive X-ray diffraction with a synchrotron radia-

tion source, indicates that both its glassy matrix structure and CuZr nano-phase are stable within a pressure range of zero to 40.8 GPa. Finally, the equation of state has been determined to be

$$-\Delta V/V_0 = 4.96\times10^{-4}+0.00868P-0.000246P^2+0.00000342P^3.$$

This work was supported by the National Natural Science Foundation of China (*50731005 and 50821001*) *and the National Basic Research Program of China* (*2010CB731600*).

1 Peker A, Johnson W L. A highly processable metallic glass: $Zr_{41}Ti_{14}Cu_{12.5}Ni_{10}Be_{22.5}$. App Phys Lett, 1993, 63: 2342–2344
2 Wang W H, Wei Q, Friedrich S. Microstructure, decomposition, and crystallization in $Zr_{41}Ti_{14}Cu_{12.5}Ni_{10}Be_{22.5}$ bulk metallic glass. Phys Rev B, 1998, 57: 8211–8217
3 Zhang T, Inoue A, Masumoto T. Amorphous Zr-Al-TM (TM =Co,Ni,Cu) alloys with significant supercooled liquid region of over 100 K. Mater Trans JIM, 1991, 32: 1005–1010
4 Li G, Gao Y P, Chi Z H, et al. Difference in microstructure of $Zr_{41}Ti_{14}Cu_{12.5}Ni_{10}Be_{22.5}$ glasses prepared in a 52 m drop tube and by water quenching. Phil Mag Lett, 2008, 88: 543–551
5 Hays C C, Kim C P, Johnson W L, et al. Composite formed by precipitation of dendritic ductile intermetallic in metallic glass. Phys Rev Lett, 2000, 84: 2901–2904
6 Zhang B Q, Jia Y Z, Wang S T, et al. Effect of silicon addition on the glass-forming ability of a Zr-Cu-based alloy. J Alloys Compd, 2009, 468: 187–190
7 Fan C, Ott R T, Hufnagel T C, et al. Metallic glass matrix composite with precipitated ductile reinforcement. Appl Phys Lett, 2002, 81: 1020–1022
8 Fan J T, Zhang Z F, Jiang F, et al. Ductile to brittle transition of $Cu_{46}Zr_{47}Al_7$ metallic glass composites. Mater Sci Eng A, 2008, 487: 144–151
9 Fan Z J, Zheng Z Y, Jiao Z B, et al. Compressive fracture characteristics of Zr-based bulk metallic glass. Sci China-Phys Mech Astron, 2010, 53: 823–827
10 Yan Z J, Yan J, Hu Y, et al. Crystallization in $Zr_{60}Al_{15}Ni_{25}$ bulk metallic glass subjected to rolling at room temperature. Sci China-Tech Sci, 2010, 53: 278–283
11 Hui X D, Liu X J, Gao R, et al. Atomic structures of Zr-based metallic glasses. Sci China Ser G-Phys Mech Astron, 2008, 51: 400–410
12 Li J F, Cao Q P, Zhou X H, et al. Microstructure of $Cu_{60}Zr_{20}Ti_{20}$ bulk metallic glass rolled at different strain rates. Sci China Ser G-Phys Mech Astron, 2008, 51: 394–397
13 Das J, Tang M B, Kim K B, et al. "Work-Hardenable" ductile bulk metallic glass. Phys Rev Lett, 2005, 94: 205501–205504
14 Cao Q P, Li J F, Zhou Y H, et al. Microstructure and microhardness evolutions of $Cu_{47.5}Zr_{47.5}Al_5$ bulk metallic glass processed by rolling. Script Mater, 2008, 59: 673–676
15 Hofmann D C, Suh J Y, Wiest A, et al. Designing metallic glass matrix composites with high toughness and tensile ductility. Nature, 2008, 451: 1085–1089
16 Chen M W, Inoue A, Zhang W, et al. Extraordinary plasticity of ductile bulk metallic glasses. Phys Rev Lett, 2006, 96: 245502–245505
17 Chen H, He Y, Shifletet G J, et al. Deformation-induced nanocrystal formation in shear bands of amorphous alloys. Nature, 1994, 367: 541–543
18 Hays C C, Kim C P, Johnson W L, et al. Microstructure controlled shearband pattern formation and enhanced plasticity of bulk metallic glasses containing in situ formed ductile phase dendrite dispersions. Phys Rev Lett, 2000, 84: 2901–2904
19 Qiu S B, Yao K F, Gong P, et al. Effects of crystallization fractions on mechanical properties of Zr-based metallic glass matrix composites. Sci China-Phys Mech Astron, 2010, 53: 424–429
20 Inoue A. Stabilization of metallic supercooled liquid and bulk amorphous alloys. Acta Mater, 2000, 48: 279–306
21 Ma L Q, Ma H A, Xiao H Y, et al. Effect of additive boron on type-Ib gem diamond single crystals synthesized under HPHT. Chinese Sci Bull, 2010, 55: 677–679
22 Han W, Jia X P, Jia H S, et al. Effects of Ti additive on HPHT diamond synthesis in Fe-Ni-C system. Chinese Sci Bull, 2009, 54: 2978–2981
23 Zang C Y, Ma H A, Xiao H Y, et al. Mechanism of diamond-to-graphite transformation at diamond-stable conditions. Chinese Sci Bull, 2009, 54: 2535–2537
24 Zhou S G, Zang C Y, Ma H A, et al. Study on growth of coarse grains of diamond with high quality under HPHT. Chinese Sci Bull, 2009, 54: 163–167
25 Li G, Jing Q, Huang L, et al. Preparation of $Zr_{60}Ni_{21}Al_{19}$ bulk metallic glass and compression behavior under high pressure. J Mater Res, 2008, 23: 2346–2349
26 Hammersley A P, Svensson S O, Hanfland M, et al. Two-dimensional detector software: From real detector to idealised image or two-theta scan. High Press Res, 1996, 14: 235–248
27 Li G, Dong Y G, Huang L, et al. High-pressure annealing effect on glass transformation temperature of $Zr_{41}Ti_{14}Cu_{12.5}Ni_{10}Be_{22.5}$ bulk metallic glass. Chin Phys Lett, 2009, 26: 086102–086105
28 Ruitenberg G, Sommer F, Sietsma J, et al. Pressure-induced structural relaxation in amorphous $Pd_{40}Ni_{40}P_{20}$: The formation volume for diffusion defects. Phys Rev Lett, 1997, 79: 4830–4833
29 Sen S, Gaudio S, Aitken B G, et al. Observation of a pressure-induced first-order polyamorphic transition in a chalcogenide glass at ambient temperature. Phys Rev Lett, 2006, 97: 025504–025507
30 Sheng H W, Liu H Z, Cheng Y Q, et al. Polyamorphism in a metallic glass. Nat Mater, 2007, 6: 192–197
31 Meade C, Hemley R J, Mao H K. High-pressure X-ray diffraction of SiO_2 glass. Phys Rev Lett, 1992, 69: 1387–1390